Humberto Peredo Fuentes* and Manfred Zehn

Application of the Craig-Bampton model order reduction method to a composite structure: MACco, COMAC, COMAC-S and eCOMAC

Abstract: The Craig-Bampton model order reduction (CB-MOR) method based on the Rayleigh-Ritz approach was applied in a previous work to simulate dynamic behavior of a composite structure (CFRP) using the modal assurance criteria (MAC) and cross orthogonality (XOR) to validate the correlation. Different coordinate modal assurance criteria are applied to complement and verify the eigenfrequencies and eigenvectors obtained of the full and reduced models using substructures (super-elements). An improvement is observed per paired mode-sensor with the MAC per coordinates criterion (MACco) in a CFRP once the stiffness parameters are updated in the full model applying a mix-numerical experimental technique (MNET) using a design of experiments (DOE). The coordinate modal assurance criteria (COMAC) and the scale COMAC (COMAC-S) results of the full models display the best results respect to the reduced model. Furthermore, slight improvement of the enhanced COMAC (eCOMAC) results are observed in the reduced model despite having lower MAC performance. This approach complements the results of the previous work using several COMAC techniques, and demostrates the feasibility to achieve low COMACs results in the reduced finite element model once the stiffness parameters of the full element model are updated. The example was prepared and solved with MSC/NASTRAN SOL103 and SDTools-MATLAB for comparative purposes.

Keywords: CBMOR; AMLS; Modal Analysis; Composites; MAC; MACco; COMACs

*Corresponding Author: Humberto Peredo Fuentes: Institute of Mechanics, Technical University Berlin, Strasse des 17. Juni 135, 10623 Berlin, Germany; Email: hperedo@mailbox.tu-berlin.de
Manfred Zehn: Institute of Mechanics, Technical University Berlin

1 Introduction

Many techniques have been proposed to obtain reduced order finite element models (known as model order reduction (MOR) methods) by reducing the order of mass and stiffness matrices of structures made of conventional [1–15] or carbon fiber reinforced polymer (CFRP). The Craig-Bampton model order reduction (CBMOR) method based on the Rayleigh-Ritz approach implemented in [3] was performed in [17] to simulate the dynamic behavior of a CFRP. The simulation of the dynamics of the CFRP was divided into two steps: a mix-numerical experimental technique [18, 19] (MNET) and the reduced model using the CBMOR method. In the first part several techniques were combined using a design of experiments [22, 33] (DOE): experimental results [20], parametric curve-fitting [10], computed FEM results, and the modal assurance criteria [21] (MAC) to obtain the stiffness parameters in a composite assembly (CFRP). The obtaining of the stiffness parameters of a CFRP is one of the most challenging problems in experimental analysis. The second part was setting the reduced model using the CBMOR, superelements, the automated multi-level substructuring [14] (AMLS) and the residual iteration [13] methods implemented in SDTools [3] once the stiffness parameters were obtained. It is documented in the literature that the combination of CBMOR, AMLS, and residual mode effects can improve the accuracy of the original transformation matrix [3, 7, 15]. This study is based on the stiffness parameters obtained in [17] with the MNET and it is an extension to validate the MAC and XOR results of the full and reduced models using different coordinate modal assurance criterias. The application of these criterias to a CFRP is not documented in the literature. The different modal assurance criterias used in this study are introduced in sections 2-6, and are implemented in SDTools. In section 7 the results are discussed.

2 Modal Correlation Criterion

There are two general categories for correlation criteria: the eigenfrequencies and eigenvectors [21]. The modal assurace criteria [23] (MAC) is one of the most useful comparison methods that relies on the eigenvector information, see Eq. (1):

$$MAC(i) = \frac{\left| \left(\sum_{j=1}^{l} (c_j\phi_{id})^H (c_j\phi_k) \right) \right|^2}{\left| \sum_{j=1}^{l} (c_j\phi_{id})^H (c_j\phi_{id}) \right| \left| \sum_{j=1}^{l} (c_j\phi_k)^H (c_j\phi_k) \right|} \quad (1)$$

where $c_j\phi_{id}$ is the jth mode shape at sensors and $c_j\phi_k$ is the jth analytical mode shape. The MAC value of 1 corresponds to an absolute correlation. The less this value becomes, the worst the eigenvector correlation will be. In the modal community a MAC coefficient of a magnitude larger or equal than 0.90 in the diagonal and less or equal than 0.05 in the off-diagonal implies a satisfactory correlation.

3 Coordinate modal assurance criterion

The coordinate modal assurance criteria (COMAC) is an extension of the MAC developed by Lieven and Ewins [24]. The implementation of the COMAC criterion requieres two stages of calculation. In the first stage, the modes from the two sets are matched using the MAC. After constructing the set of *NM* mode pairs to be correlated, the second stage of the COMAC is the calculation of the correlation values at each coordinate, over all the correlated pairs [25], see Eq. (2):

$$COMAC_{(l)} = 1 - \frac{\left| \left(\sum_{j=1}^{NM} (c_l\phi_{jA})(c_l\phi_{jB}) \right) \right|^2}{\left| \sum_{j=1}^{NM} (c_l\phi_{jA}) \right|^2 \left| \sum_{j=1}^{NM} (c_l\phi_{jB}) \right|^2} \quad (2)$$

where $c_l\phi_{jA}$ is the jth mode shape at sensors and $c_l\phi_{jB}$ is the jth analytical mode shape selected. It is important to note that the modes have to be normalized as this gives equal weighting to all modes. Unfortunaly, the standard COMAC cannot identify differences that occur due to fairly common ploblems during modal testing. These problems include orientation of the accelerometers and transducers scale factor errors [26]. Additionally, the COMAC is equally sensitive to large and small motion of DOF, which can make COMAC results more difficult to interpret. COMAC values closer to zero per DOF represent a higher agreement.

4 Scale coordinate modal assurance criterion

The scale coordinate modal assurance criterion (COMAC-S) is computed with shapes in set B scaled using the modal scale factor (MSF) [3, 23] (see Eq. (3)). The MSF provides a qualitative way of comparing two modal vector sets. This criterion has been used by Ewins [21], Allemang [23], Catbas [25], and Balmés [3] for a variety of different analyses including structural modifications and frequency response function (FRF) synthesis for comparison with experimental data [32].

$$COMAC - S_{(l)} = 1 - \frac{\left| \left(\sum_{j=1}^{NM} (c_l\phi_{jA})(c_l\hat{\phi}_{jB}) \right) \right|^2}{\sum_{j=1}^{NM} \left| (c_l\phi_{jA}) \right|^2 \sum_{j=1}^{NM} \left| (c_l\hat{\phi}_{jB}) \right|^2}$$

$$(c_l\hat{\phi}_{jB}) = (c_l\phi_{jB})MSF = (c_l\phi_{jB})\frac{(c_l\phi_{jB})^T(c_l\phi_{jA})}{(c_l\phi_{jB})^T(c_l\phi_{jB})}$$

$$(3)$$

This COMAC-S criterion sets the scaling of vectors in set B to minimize the quadratic norm of the difference between $(c_l\phi_{jA})$ and $(c_l\hat{\phi}_{jB})$ [3]. Scaling assumes that each experimental mode shape is already correlated with an analytical shape. When two modal vectors are scaled similarly, elements of each vector can be averaged, differentiated or sorted to provide an indication of the type of error vector superimposed on the modal vector [27]. The lower values of the COMAC-S represent also a higher agreement per DOF.

5 Enhanced coordinate modal assurance criterion

The formulation of the enhanced COMAC (eCOMAC), introduced by Hunt [26], overcome some of the limitations of the standard COMAC, expressed as:

$$eCOMAC_{(l)} = \frac{\sum_{j=1}^{NM} \left\| (c_l\tilde{\phi}_{jA}) - (c_l\hat{\phi}_{jB}) \right\|}{2NM} \quad (4)$$

The comparation is done using mode shapes that are vector normalized to 1 and there must be phase correlation

between pair modes, see Eq. (5)

$$(c_l \tilde{\phi}_{jA}) = \frac{(c_l \phi_{jA})}{\|c_l \phi_{jA}\|} \tag{5}$$

This can be accomplished by examining the high coefficient DOF in the mode pairs or by using the MSF to determine if the normalization mode should be multiplied by −1. The use of eCOMAC requires this extra step in mode shape normalization, namely a check for phase consistency between each mode pair using the MSF [26]. The unit normalization and correct phasing are interpreted in the same way as the COMAC. The eCOMAC values are obtained from zero to one, similar to COMAC, where a value closer to zero per DOF will have a higher correlation agreement. Furthermore, Hunt reported in [26] that the eCOMAC can successfully identify measurement errors such as scaling and polarity. This is because the eCOMAC is less sensitive to errors at small motion of DOF and it is considered more robust than the standard COMAC.

# 6 Modal assurance criteria per pair-sensor (MACco)

The MAC per pair-sensor (MACco) criterion consists in the sequential order of sensors that contribute most to the poor correlation. The MACco is known with different names in the literature: the MAC coordinate criterion [3] or the MAC variation technique [28]. It is an iterative algorithm that takes the modes in $c_j \phi_{id}$ and $c_j \phi_k$ and computes the pair MAC with one sensor "removed" that contribute to low MAC values. The MACco algorithms leads to the best mean MAC for the paired modes, and is a direct indication of where the poorest correlation is located. In this work is suggested the possibility of applying the MACco criterion implemented in [3] to identify the improvement per pair-sensor using the updated stiffness parameters of the FE model obtained in [17].

7 Results

A summary of the results in [17] is introduced to present the initial COMAC results from this study. All the measurements were performed with the Scanning Laser Doppler Vibrometer (SLDV) PSV840 by suspending the CFRP component from very soft cords (free condition), (see Fig. 1), provided by the DLR Braunschweig. The shaker LDS V406 and the stinger with length of 65 mm at node 17 are used to
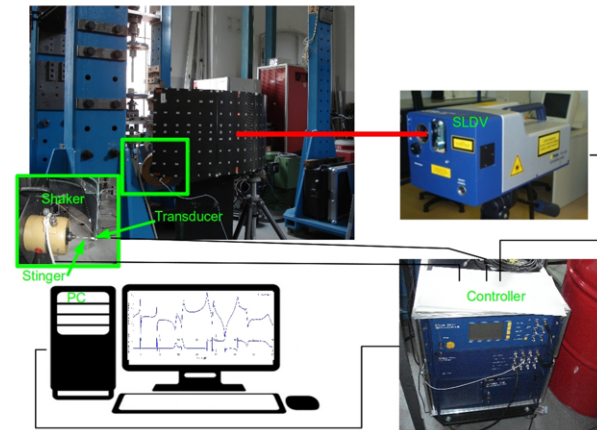
(a)
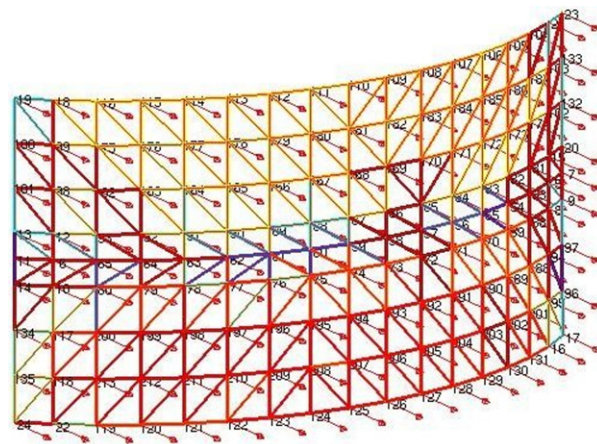
(b)
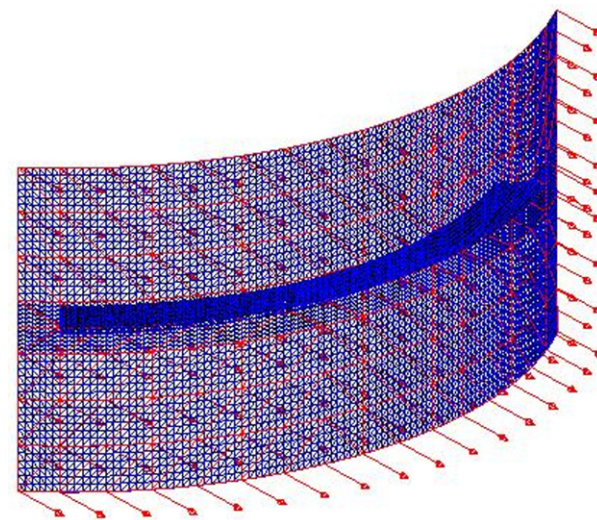
(c)

Figure 1: Experiment: a) Experimental set-up; b) 153 Y-direction sensors; c) 153 sensors in the FEM model [17].
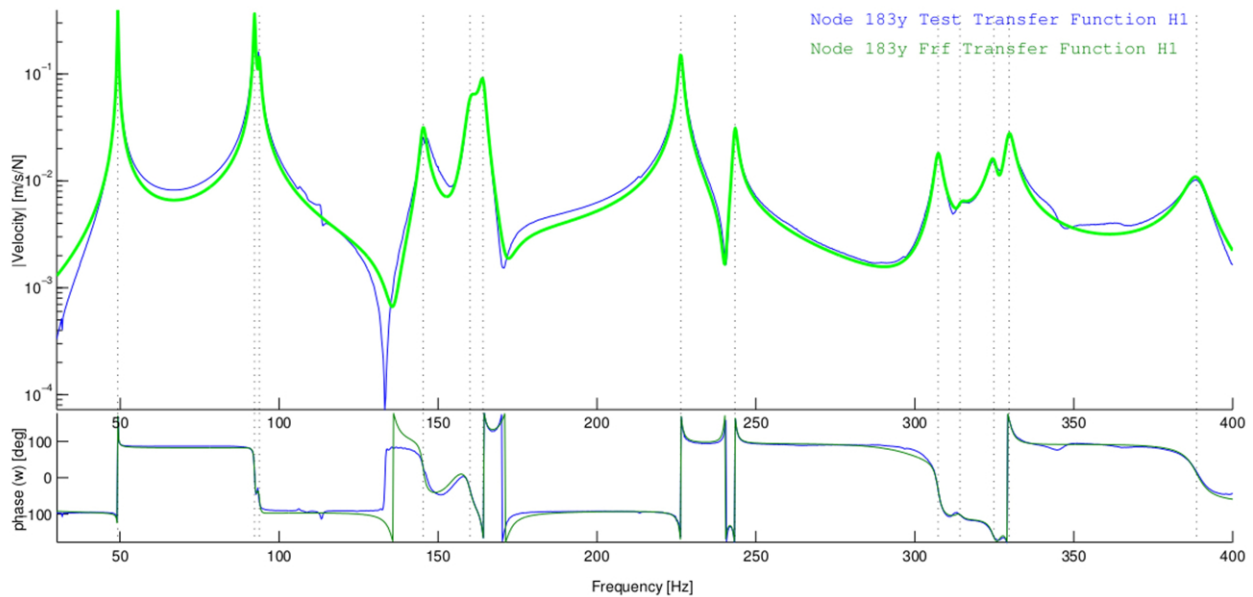
Figure 2: FRF (blue) and fitting curve (green) of composite model at node 183y [17].

excite the structure that produce a sinusoidal vibration velocity signal on the line of sight of the SLDV (out-of-plane). The reason to use a stinger is to ensure that the shaker will only impart force to the structure along the axis of the stinger. The excitation signal selected is a periodic chirp (with frequency span 30–400 Hz, 6400 lines of resolution, with complex average type and number of average per Frequency Response Function (FRF) equal to 10), and reflective foil is used to acquire the response measurement location. The input force is measured using a force transducer Dytran 1051V3 and power amplifier LDS PA 100 in order to record the excitation in the transverse direction.

The interpolation between the experimental measurements uses FRFs [10]. The FRF, (see Fig. 2), allowed us to compare the experimental modal parameters (frequency, damping, and mode shape) with the FE model. The Fast Fourier Transform (FFT) is a fundamental procedure that isolates the inherent dynamic properties of a mechanical structure and in our case with respect to the full and reduce FE model performed in [17].

To approximate the measurements (blue line) through a polynomial function (green line), we used the frequency domain identification of structural dynamics applying the pole/residue parameterization [10], (see Fig. 2). The correlation results vs the experimental model was performed at low frequency (up to 400 Hz), based on the curve-fitting generated from the experimental measurements [10]. A bandwith of 2% is used to localize the eigenfrequencies.

The MAC analysis of the full and reduced FE models obtained in [17] can be observed in Fig. 3 (MATLAB,

NASTRAN, and CBMOR model respectively) versus the experimental measurements. Two different elements and solvers were used for reference purposes: CTRIA3 shell (from MSC/NASTRAN) and pshell (from SDTools) [29, 30]. The same number of modes were calculated for both the full and reduced FE models, using super-elements. Cross orthogonality MAC (XOR) was performed to verify the approximation of the MOR in low frequency range (12 mode pairs) versus the full model, see [17].

A good MAC correlation was obtained between the three models and the MAC results displayed an agreement with the literature (the MAC results in the reduced FE model are slightly lower). These MAC results of the full FE models were calculated with the stiffness parameters obtained in [17] performing a DOE full factorial in MINITAB [33]. The nearly double correlation in the experimetal results identified in Fig. 3 and Table 1 for the full and reduced models suggest the presence of the veering phenomena [16, 31] (bending and torsional mode at the same frequency) in our composite component assembly. Thus, lower MAC results in 4, 9, 10 and 11 paired modes (see Fig. 3b) and 5, 9, 10 and 11 paired modes (see Fig. 3c) were archieved and identified using the experimental results.

Furthermore, the reduced model was performed using CMS in terms of substructure /super-element technique, AMLS and residual iteration methods implemented in [3]. The reduced model was built up defining two super-elements.
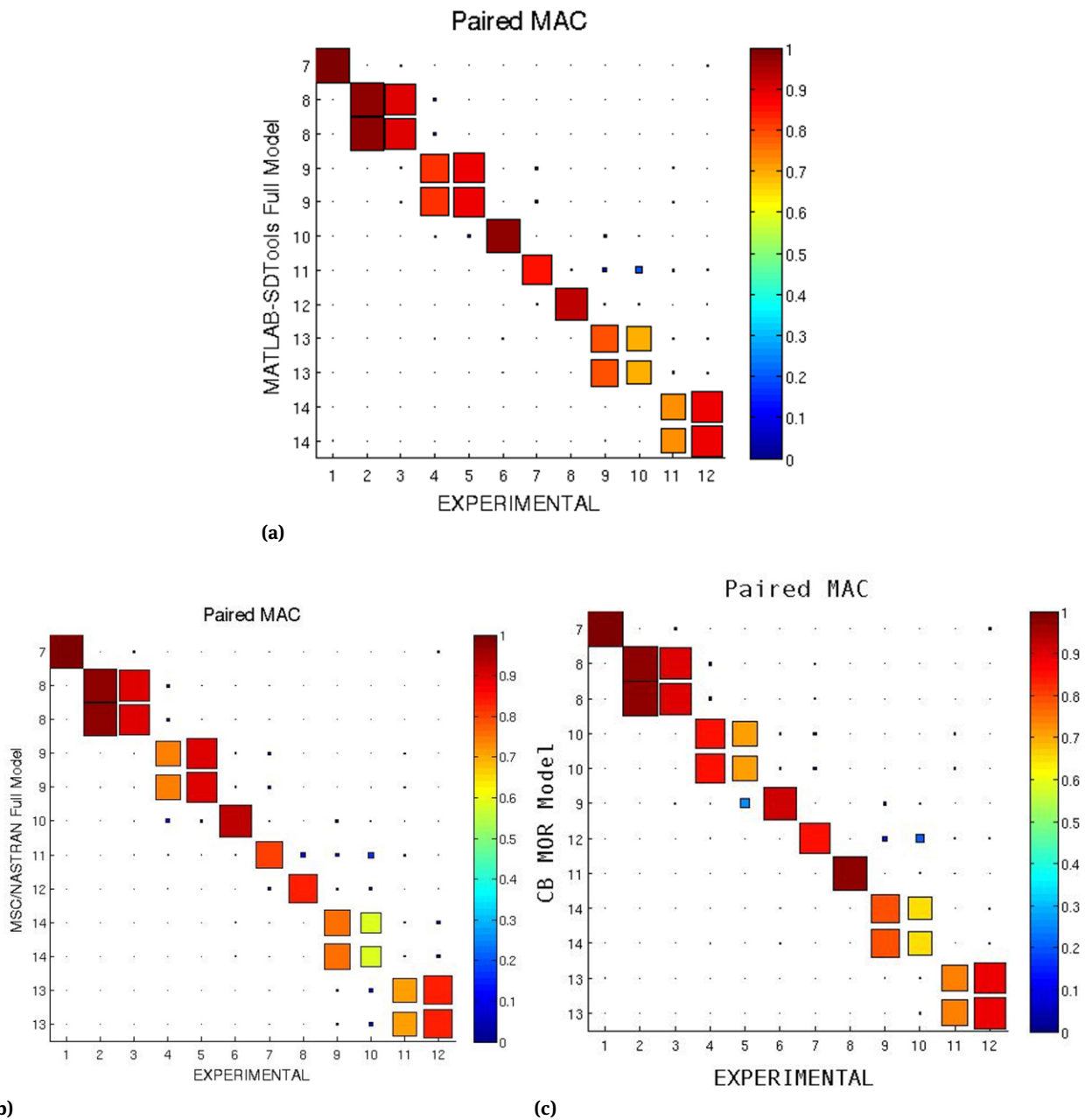
(a)

(b)

(c)

Figure 3: Comparative MAC: a) SDtools-Exp, b) MSC/NASTRAN-Exp, c) CBMOR-Exp [17].

Super-element 1 has 4,753 nodes and 9,219 elements, while super-element 2, has 1,615 nodes and 3,026 elements. The defined super-elements shared 579 DOF distributed in 123 nodes along the common border with different DOF per node, according to the CMS that has defined an appropriate [T] matrix [3]. Some mode shapes of the reduced and full models can be observed (see Fig. 4) as well as experimental measurements (see Fig. 5).

After constructing the set of NM mode pairs, the next step is the calculation of the COMAC values over all the correlated mode pairs, as given in the Eq. (2). Different CO-

MAC results (in blue) can be visualized in Fig. 6 (MATLAB (non-updated), MATLAB (updated), NASTRAN (updated), and CBMOR model, respectively) with respect to the number of sensors (x-axis). Fig. 6a is included as a reference to visualze the improvement between the FE models using the different COMACs. The COMAC values are calculated and displayed an improvement after updating the material properties with similar pattern and values between FE models, (see Figs. 6b, 6c, 6d). The best COMAC result of the full FE models are obtained on sensor 107y=0.036 ,and the worst result on sensor 201y=0.397 (see Fig. 6b). Further-
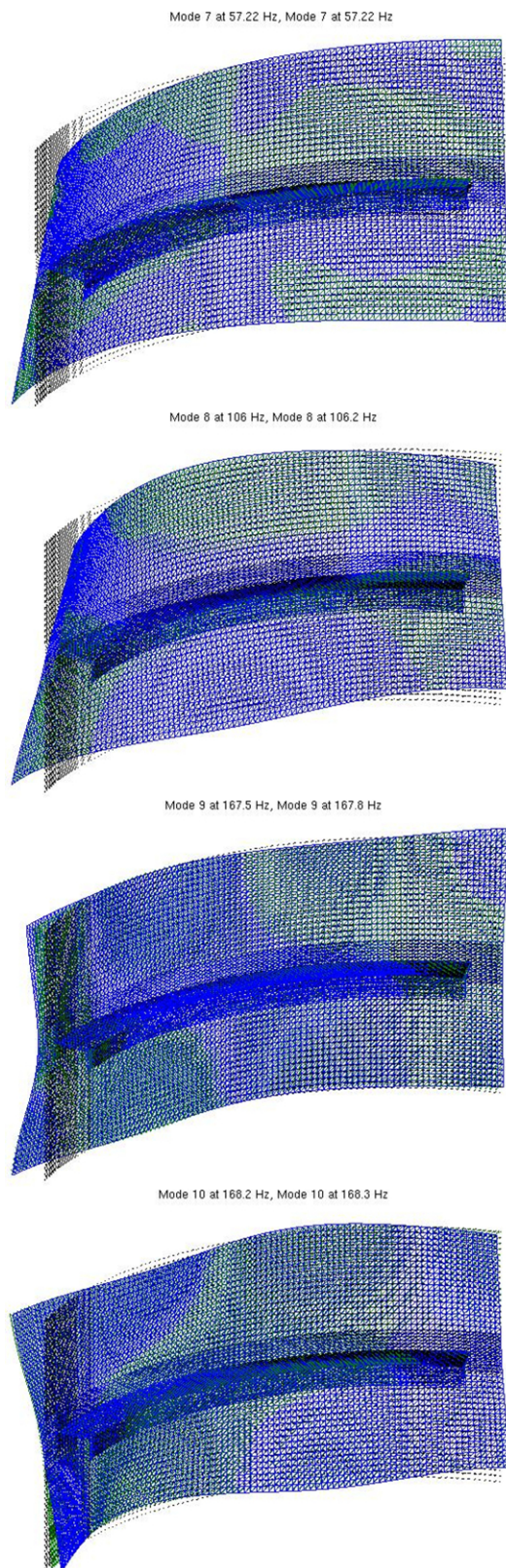
Figure 4: Full model in MATLAB (in blue) vs CBMOR (in green) [17], for values see Table 1.
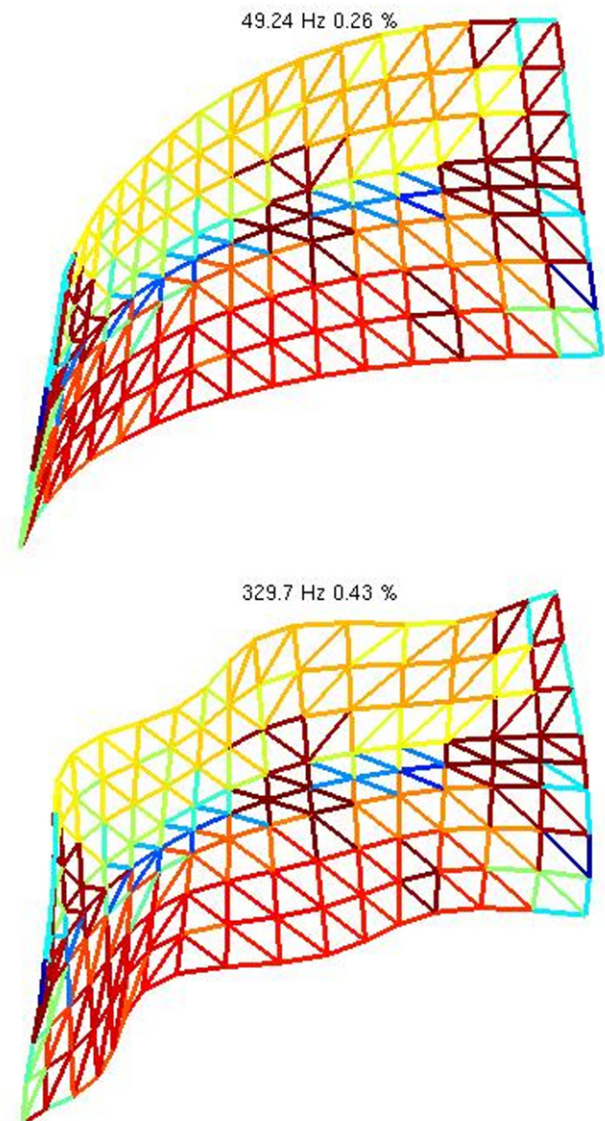
Figure 5: Experimental mode shapes [17].

more, in the reduced FE model the best and worst COMAC results are found on sensors 84y=0.052 and 201y=0.423 respectively.

A pattern in the results can be visualized using the CO-MAC criterion (see Fig. 6) with slight differences (except for the non-updated FE model). The COMAC-S results, for all the FE models, display an improvement respect to the CO-MAC values (green line). The best COMAC-S value is displayed in the full FE model in Fig. 6b on sensor 209y=0.019, and the worst value on sensor 201y=0.366. In the reduced FE model the best and the worst COMAC-S values are obtained on sensors 114y=0.026 and 201y=0.388 respectively.

The eCOMAC results (in brown) of the full and reduced FE models show a much lower values respect to the CO-MAC and COMAC-S results. The eCOMAC criterion displays
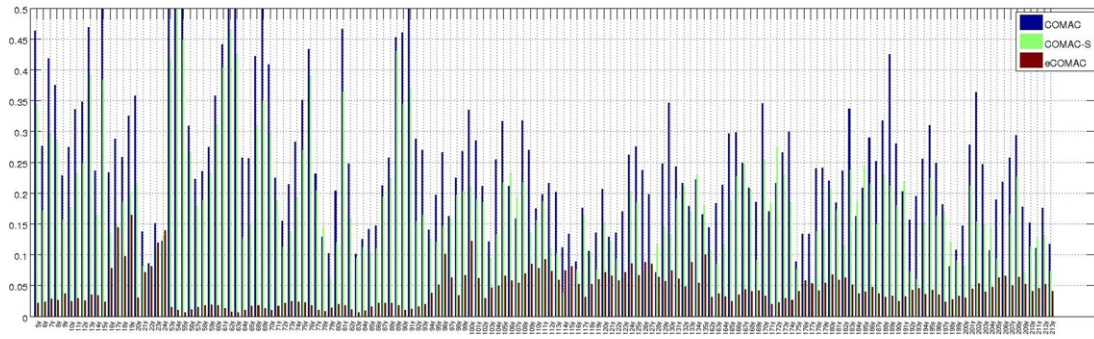
(a)
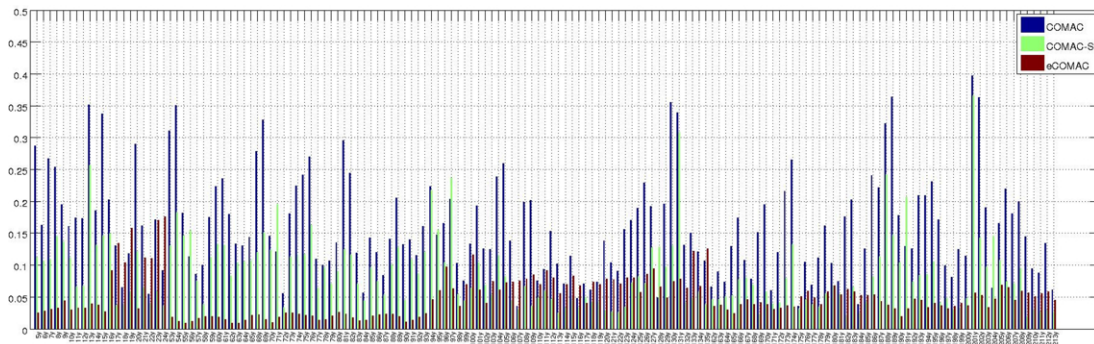
(b)
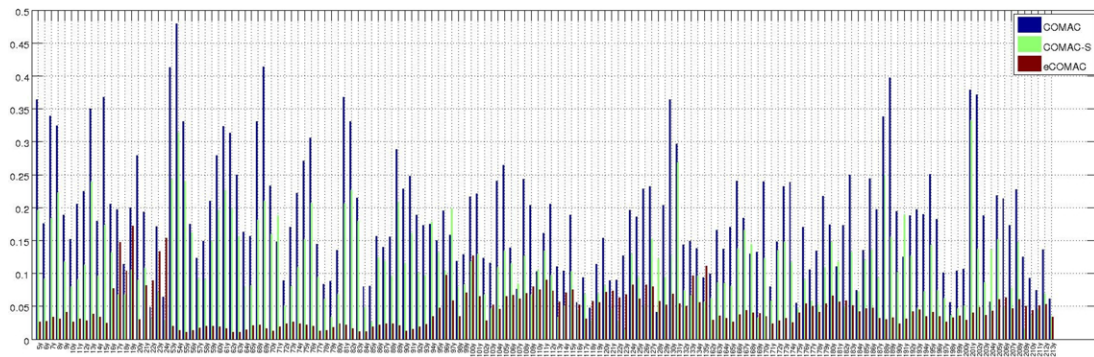
(c)
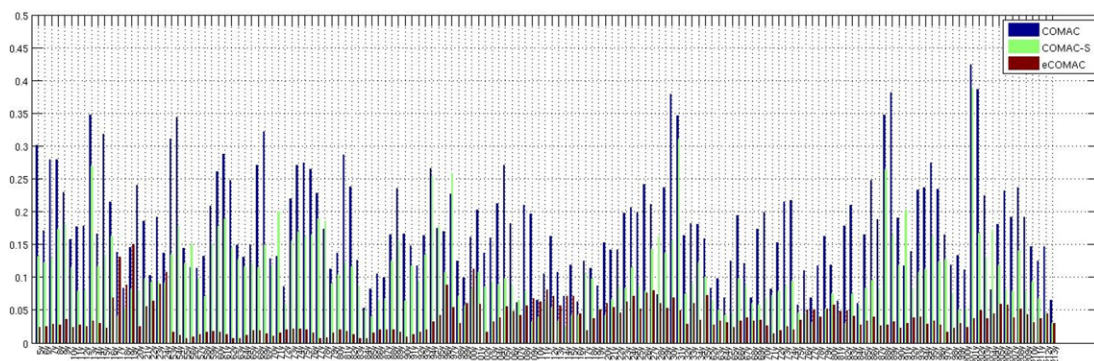
(d)

Y-SENSORS

Figure 6: Comparison of COMACs: a) SDtools-Exp (non-updated), b) SDtools-Exp(updated) c) MSC/NASTRAN-Exp (updated), d) CBMOR-Exp.

Table 1: Full and reduced model results versus experimental results [17].

#	Experimental	#	Full	DF/FA	MAC	CBMOR	DF/FA	MAC
1	49.243	7	57.218	16.2	100	57.218	16.2	100
2	92.265	8	106.02	14.9	97	106.21	15.1	97
3	93.756	8	106.02	13.1	90	106.21	13.3	90
4	145.29	10	168.20	15.8	83	168.29	15.8	84
5	160.05	10	168.20	5.1	86	168.29	5.1	71
6	164.18	9	167.50	2.0	98	167.79	2.2	92
7	226.36	12	236.83	4.6	86	236.93	4.7	85
8	243.40	11	234.99	−3.5	96	235.12	−3.4	97
9	307.33	14	323.93	5.4	81	326.82	5.4	80
10	314.18	14	323.93	3.1	66	326.82	4.0	65
11	324.83	13	315.26	−2.9	74	315.33	−2.9	74
12	329.67	13	315.26	−4.4	90	315.33	−4.3	89

the best results with the exception of few sensors (16y-19y and 21y-24y) for all the FE models. The updated full FE model shown in Fig. 6b, displays the best eCOMAC value at sensor 83y (0.009), with the worst eCOMAC value found at sensors 24y (0.176). Furthermore, in the reduced FE model the worst and the best eCOMAC values are found in the same sensors (24y=0.15 and 83y=0.006 respectively). It can be appreciated that the eCOMAC in the reduced FE model displays slightly enhanced results versus the full FE models (see Fig. 7). The lower eCOMAC values suggest a good normalization and phase correlation between pair coordinates of the full and reduced FE model with the experimental results.

The lower COMACs values obtained with different criterias suggest a good agreement of the full and reduced FE models versus the experimental measurements. It is necessary to mention the good agreement between different COMAC, COMAC-S and eCOMAC using two types of elements and solvers.

Applying the MACco criterion it is possible to analyze the paired mode per sensors ordered in ascending order leading to the best "mean MAC" for the paired modes, see Fig. 8. The MACco criterion and COMAC criteria also display a significant improvement per mode paired-sensor, which contribute to high MAC values using the stiffness parameters obtained in [17]. The "mean MAC" (represented as a solid line in blue in Fig. 8) is obtained by calculating the mean of the MAC per mode paired-sensor selected of each FE model. The x-axis of each graph in Fig. 8 represents the total number of sensors (153 sensors) used with the MACco algorithm. Only the worst ten MAC results per paired mode-sensor of each FE model are displayed in Tables 2 and 3.

Table 2 is divided into three sections, displaying the MACco results of the non-updated and updated full FE models respectively. The values of the "mean MAC" can be observed in Table 2 of each FE model. In Table 3 the MACco results of the reduced model are displayed. In both tables an improvement using the updated stiffness parameters is observed. Before updating the material properties, the sensors 16y displays the worst "mean MAC" = 77. After updating the stiffness parameters, the sensors 16y shows a considerable improvement when applying the MACco criterion in the full and reduced models ("mean MAC" of 88, 85 and 87 respectively). The worst paired mode per sensor is identified in the pair number 16 of each updated FE model (MAC per paired-sensor of 67, 60, 67 respectively) on sensor 16y. The worst paired mode per sensor of the non-updated FE model is identified in the pair number 10 on the sensor 16y with "mean MAC" value of 58. With the exception of the sensors 104y and 133y in Tables 2 and 3, the worst MACco results in the updated FE models are identified in the same sensors, (see Fig. 9), per paired mode on the edge of the CFRP.

8 Conclusions

The results have shown a good correlation in dynamic behavior of the composite component assembly model using the pshell and CTRIA3 elements applying different solvers for comparative purposes in the FE models. The MAC values obtained (eigenfrequencies and eigenvectors) for the full and reduced FE models versus the experimental measurements in the previous work are consistent applying different coordinate criteria (COMACs and MACco). The im-

**Table 2:** MACco results - Full models versus experimental results.

Pair number		7	8	9	10	11	12	13	14	15	16	17	18
Experimental		1	2	3	4	5	6	7	8	9	10	11	12
SDTools FEM (non-updated)		7	8	8	9	9	10	12	11	14	14	13	13
Sensor	Mean MAC												
All	77	99	97	90	58	87	73	65	63	73	61	72	86
16y	77	99	97	91	57	87	73	65	63	73	62	75	87
23y	78	99	97	92	62	88	71	69	59	72	63	74	86
21y	78	99	97	93	66	89	70	71	57	72	63	74	87
129y	78	99	97	93	65	89	70	70	58	72	65	75	88
96y	79	99	97	93	64	89	70	70	60	73	66	76	88
95y	79	99	97	94	64	89	71	70	60	73	66	77	88
17y	79	99	97	94	62	90	72	68	63	73	66	78	90
128y	80	99	97	94	61	89	73	68	63	73	68	79	90
133y	80	99	97	94	64	90	71	70	60	73	69	79	90
104y	80	99	97	95	66	90	71	70	61	74	69	79	90
Experimental		1	2	3	4	5	6	7	8	9	10	11	12
SDTools FEM (updated)		7	8	8	10	10	9	12	11	14	14	13	13
Sensor	Mean MAC												
All	87	100	97	90	83	86	98	86	96	81	66	74	90
16y	88	100	97	91	83	86	98	86	96	82	67	76	90
96y	88	99	97	91	82	87	98	87	97	83	69	77	90
95y	88	100	97	91	82	87	98	88	97	84	70	78	90
23y	89	99	97	92	84	87	97	88	96	84	73	77	90
131y	89	100	97	93	85	88	97	89	96	85	73	77	90
17y	89	100	97	93	84	89	97	89	97	85	74	78	91
21y	90	100	97	94	85	89	97	89	97	85	76	78	91
129y	90	100	97	94	85	89	97	89	97	86	77	79	92
128y	90	100	97	94	84	89	97	89	97	86	79	80	92
97y	91	100	97	94	84	89	97	90	97	87	79	81	92
Experimental		1	2	3	4	5	6	7	8	9	10	11	12
MSC/NASTRAN FEM (updated)		7	8	8	9	9	10	11	12	14	14	13	13
Sensor	Mean MAC												
All	83	100	97	90	74	90	93	81	84	76	59	71	84
16y	84	99	97	91	74	91	93	81	85	77	60	74	84
23y	84	99	97	92	77	91	92	82	83	76	63	73	84
96y	85	99	97	92	76	92	93	82	84	77	64	74	85
21y	85	99	97	93	79	92	92	83	83	77	65	74	85
95y	85	100	97	93	79	92	92	84	83	78	66	74	85
17y	86	100	97	93	77	93	93	83	85	78	67	76	87
129y	86	100	97	93	77	93	93	82	85	78	68	78	88
131y	86	100	97	94	77	93	93	83	86	79	69	78	88
128y	87	100	97	94	76	93	93	83	86	80	71	79	88
133y	87	100	97	95	79	93	93	84	85	80	72	78	88
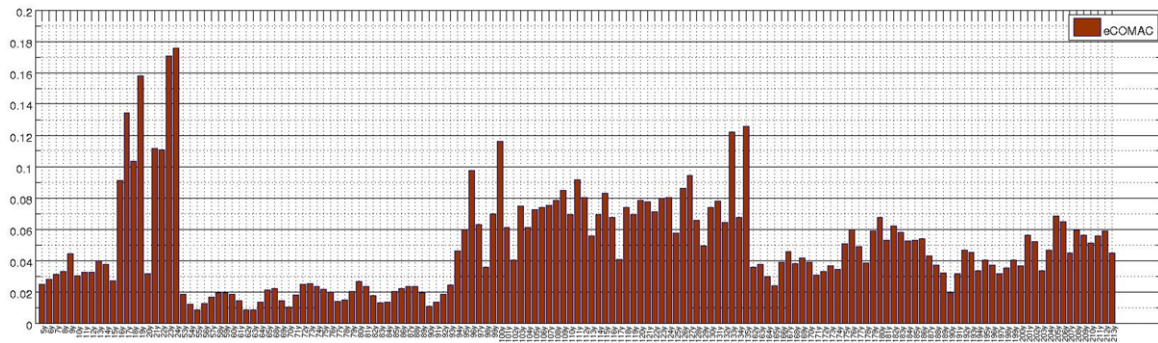
(a)
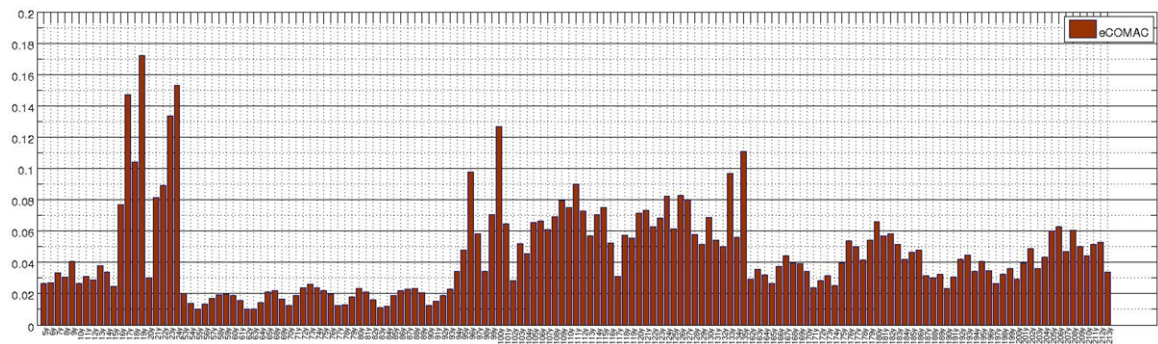
(b)
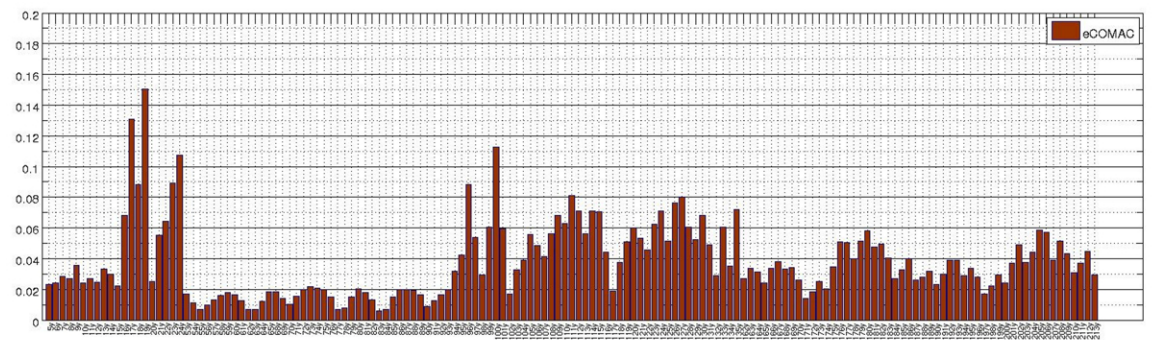
(c)

Y-SENSORS

Figure 7: Comparison of eCOMACs: a) SDtools-Exp(updated) b) MSC/NASTRAN-Exp (updated), c) CBMOR-Exp.

provement of the COMACs results is observed in all the FE models once the stiffness parameters were updated. The full FE model with pshell elements displays the best CO-MAC, COMAC-S and MACco results between full FE models. The reduced model obtained by means of the Craig-Bampton MOR method (the reduced model has 123 nodes with 2 substructures and 579 DOF) has demonstrated a good agreement with the experimental results using different COMACs. The eCOMAC values of the reduced model present a slight enhancement in the results and are the best values versus the eCOMAC results obtained in the

full models. The MACco results of the reduced FE model also show a good agreement with the experimental measurements with respect to the full FE model. The experimental results performed with an SLDV and the identification of pole/residues used are suitable to validate the dynamic analysis of CFRP using coordinate assurance criteria applying modal order reduction. In order to achieve high quality COMACs results in the FE models that can adequately capture the dynamic behavior, the material properties were updated by applying a DOE and are crucial in the MOR correlation with the experimental results. The
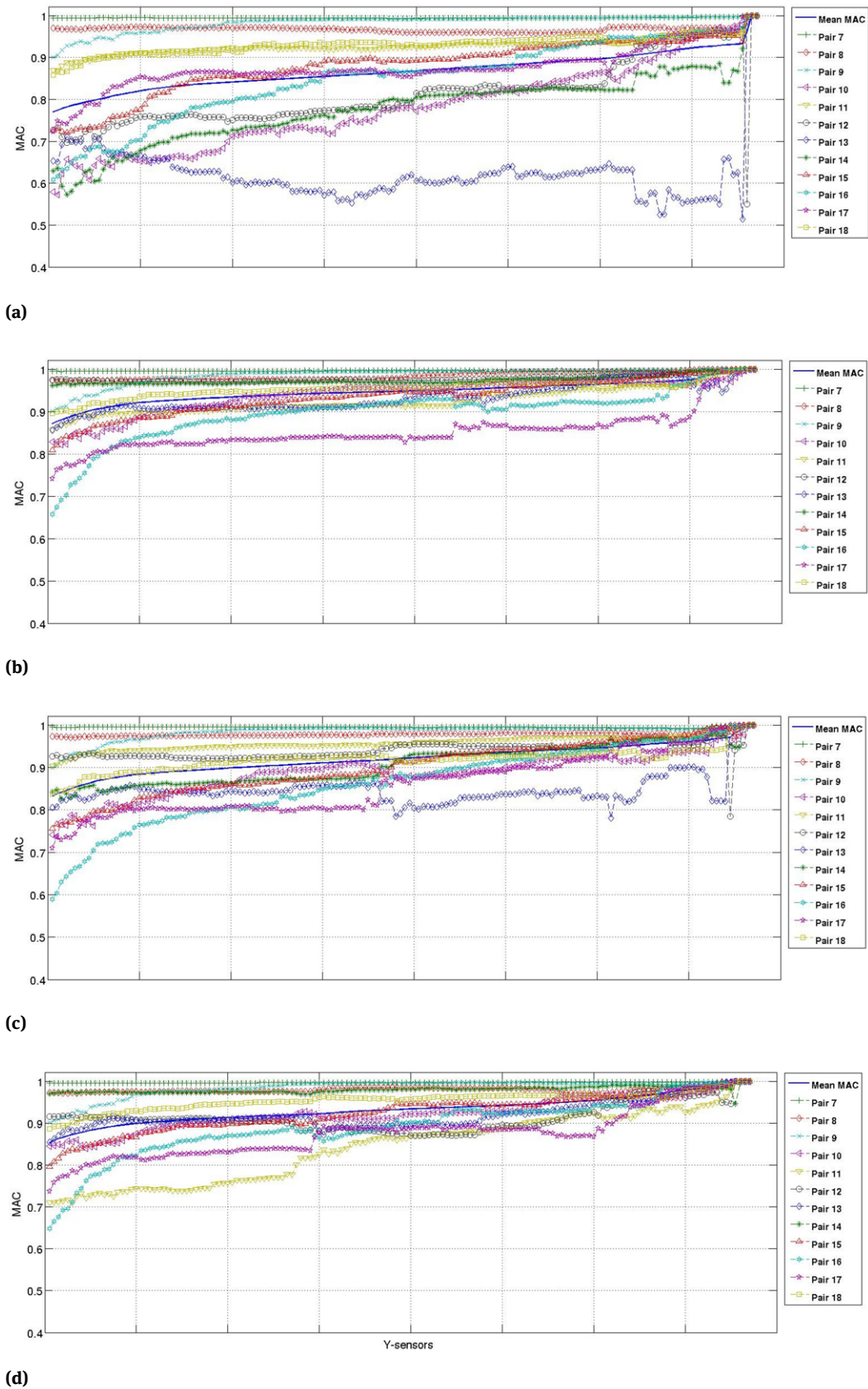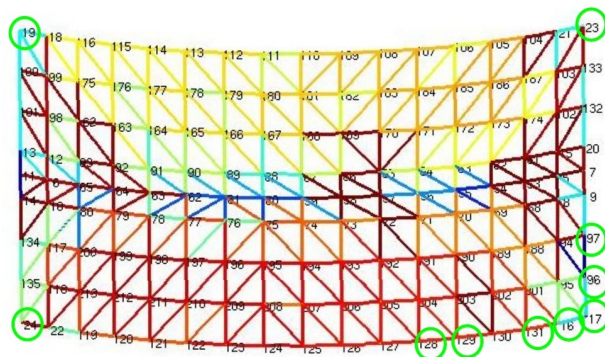
(a)

(b)

(c)

(d)

Figure 8: Comparison of MACcos: a) SDtools-Exp (non-updated), b) SDtools-Exp (updated), c) MSC/NASTRAN-Exp (updated), d) CBMOR-Exp.

Table 3: MACco results - Reduced model versus experimental results.

Pair number		7	8	9	10	11	12	13	14	15	16	17	18
Experimental		1	2	3	4	5	6	7	8	9	10	11	12
Reduced FE model CBMOR		7	8	8	10	10	9	12	11	14	14	13	13
Sensor	Mean MAC												
All	85	100	97	90	84	71	92	85	97	80	65	74	89
16y	86	100	97	91	85	71	92	86	97	81	67	76	89
95y	86	100	97	91	85	71	92	87	97	82	68	77	89
96y	87	100	97	91	85	71	92	88	97	83	69	77	89
131y	87	100	97	92	86	72	92	89	98	83	70	77	89
129y	87	100	97	92	86	71	92	88	98	84	71	79	89
23y	87	100	97	93	86	72	91	88	97	84	73	78	90
17y	88	100	97	93	85	73	91	88	97	84	74	79	91
128y	88	100	97	93	84	72	92	89	97	85	76	80	91
21y	88	100	97	94	84	73	91	89	97	85	77	80	91
97y	88	100	97	94	84	73	91	90	97	85	78	80	92

Figure 9: Identification of the "worst Y-sensors" (green) using MACco.

MAC using superlements, the AMLS and residual iteration methods implemented in SDTools that show a good normalization and phase correlation with the experimental results.

It is needed to perform an assesment with other elements of similar characteristics for accuracy and sensitivity purposes applied to different CFRP. Different mode shape expansion methods of coupled predictions consisting of local FE model, enhanced AMLS, classical theory of structural modification by coupling, and CMS with interface model order reduction should be assessed for future work to validate the MNET results.

COMACs and MACco results obtained in full and reduced FE models based on the Rayleigh-Ritz approach to simulate dynamic behavior of a CFRP assembly suggest the following conclusions. A high accuracy in the updated stiffness parameters obtained that might be used to verify the mechanical properties, such as the Poisson ratio, along the measured CFRP. The updated mass and stiffness matrices in the full model played an important roll in the MNET procedure to perform the CBMOR method. The identification of the veering phenomena in the CFRP component assembly looked at the full and reduced FE models using the MAC. The application of the MACco to identify the improvement per pair-sensor once it was updated the FE model. The validation of the correlation proved applying different COMACs based on the type of finite elements used. Finally, the slightly improvement of the transformation matrix of the reduced model observed in the eCO-

References

[1] Hurty W.C., Dynamic analysis of structural systems using component modes, AIAA J., 3(4), 1965, 678–685

[2] Craig R.J., Bampton M., Coupling of substructures for dynamic analyses, AIAA J., 6(7), 1968, 1313–1319

[3] Balmès E., Structural dynamics toolbox and FEMLink, User's Guide, SDTools, Paris, France, 2016, http://www.sdtools.com/help/sdt.pdf

[4] Van der Valk P.L.C., Model Reduction & interface modeling in dynamic substructuring, MSc. thesis, TU Delf, Netherlands, 2010.

[5] Reddy J. N., Mechanics of Laminated Composite Plates and Shells: Theory and Analysis, CRC, Press Second edition, 2004

[6] Cunedioğlu Y., Muğan A., Akçay H., Frequency domain analysis of model order reduction techniques, Finite Elements in Analysis and Design, 42, 2006, 367–403

[7] Balmès E., Optimal Ritz vectors for component mode synthesis using singular value decomposition, AIAA J., 34(5), 1996, 1256–1260

[8] Balmès E., Use of generalized interface degrees of freedom in component mode synthesis, IMAC 1996, 204–210

[9] Balmès E., Efficient Sensitivity Analysis Based on Finite Element Model Reduction, IMAC 1997, 1–7

[10] Balmès E., Frequency domain identification of structural dynamics using the pole/residue parametrization, IMAC 1996, 540–546

[11] Balmès E., Review and Evaluation of shape expansion methods, IMAC 2000, 555–561

[12] Balmès E., Modes and regular shapes. How to extend component mode synthesis theory, XI DINAME, 28th February-4th March 2005, 1–14

[13] Bobillot A., Balmès E., Iterative computation of modal sensitivities. AIAA J., 44(6), 2006, 1332–1338

[14] Kaplan M., Implementation of Automated Multilevel Substructuring for frequency response Analysis of structures, PhD thesis, The University of Texas at Austin, U.S.A.

[15] Jin-Gyun K., Seung-Hwan B., Phill-Seung L., An enhanced AMLS method and its performance. Computed methods in applied mechanics and engineering, 287, 2015, 90–111

[16] Bonisoli E., Delprete C., Espoito M., Mottershead J. E., Structural Dynamics with conicident Eigenvalues: Modeling and Testing, Modal Analysis Topics, 3, Conferencing Proceedings of the Society for Experimental Mechanics Series 6, 2011, 325–337

[17] Peredo Fuentes H., Zehn M., Application of the Craig-Bampton model order reduction method to a composite component assembly, Facta Universitatis, series: Mechanical Engineering, 12(1), 2014, 37–50

[18] Meuwissen M.H.H., An inverse method for the mechanical characterization of metals, PhD thesis, Technische University Eindhoven, Netherlands, 1998

[19] Van Ratingen M.R., Mechanical identification of inhomogeneous solids, PhD thesis, Technische University Eindhoven. Netherlands, 1994

[20] Gade S., Møller N.B., Jacobsen N.J., and Hardonk B., Modal analysis using a scanning laser Doppler vibrometer, Sound and Vibration Measurements A/S, 2000, 1015–1019

[21] Ewins D. J., Modal testing: Theory and practice, Research Studies Press, Letchworth, U. K., 1995

[22] Montgomery D. C., Design and analysis of experiments, 5th ed., John Wiley & Sons Inc., USA, 2000

[23] Allemang R.J., Brown D.L., A correlation coefficient for modal vector analysis, IMAC 1982, 110–116

[24] Lieven N. A.J., Ewins D.J., Spatial correlation of mode shapes, The coordinate modal assurance criterion *(COMAC)*, IMAC 1988, 690–695

[25] Catbas F.N., Aktan A.E., Allemang R.J., Brown D.L., Correlation function for spatial locations of scaled mode shapes (COMEF), IMAC 1998, 1550–1555

[26] Hunt D.L., Application of an enhanced coordinate modal assurance criteria (ECOMAC), IMAC 1992, 66–71

[27] Allemang R.J, The modal assurance criterion – twenty years of use and abuse, Sound and vibration, 2003, 14–21

[28] Brughmans M., Leuridan J., Blauwkamp K., The application of FEM-EMA correlation and validation techniques on a body-in-white. IMAC 1993, 646–654

[29] Batoz J.L., Bathe K.J., Ho L.W., A Study of three node triangular plate bending elements, International Journal for Numerical Methods in Engineering, 15, 1980, 1771–1812

[30] Batoz J.L., Lardeur P., Composite plate analysis using a new discrete shear triangular finite element, International Journal for Numerical Methods in Engineering, 27, 1989, 343–359

[31] Pierre C., Mode Localization and eigenvalue loci of Bridges with Aeroeslastic effects, Journal of Engineering Mechanics 126(3), 1988, 485–502

[32] Schwarz B., Richardson M., Scaling mode shapes obtained from operating data, IMAC 2003, 1–8

[33] Minitab 17 Statistical Software, Computer software, State College, PA:Minitab, Inc., 2010, (www.minitab.com)